Atmospheric
Chemistry
and Physics

Supplement of

Distinctive aerosol–cloud–precipitation interactions in marine boundary layer clouds from the ACE-ENA and SOCRATES aircraft field campaigns

Xiaojian Zheng et al.

*Correspondence to:* Xiquan Dong (xdong@arizona.edu)
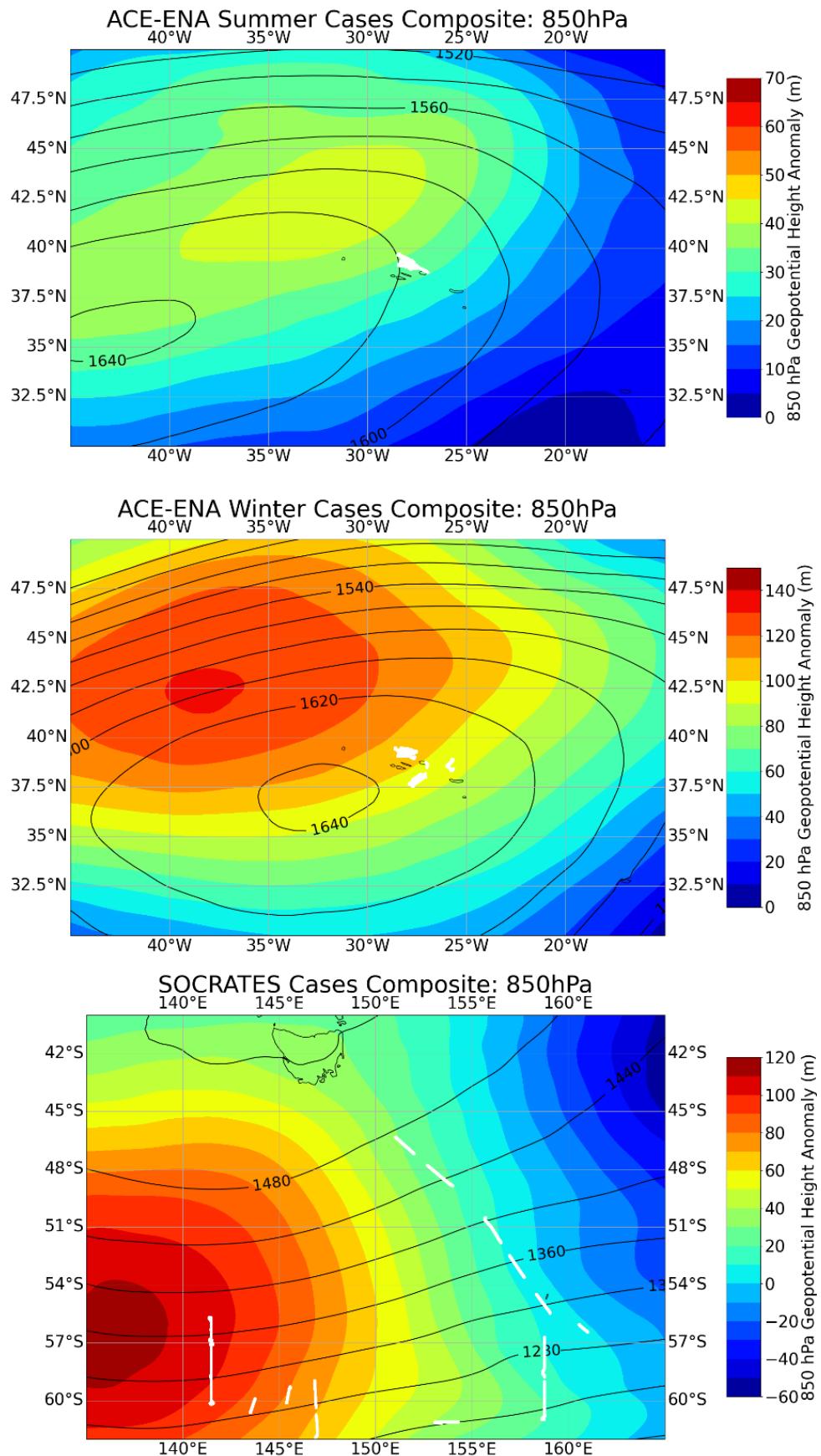
Figure S1. The selected-cases 850 hPa geopotential height composite (black contours), and the height anomaly from (shaded area) the 20-year climatology (2000-2020), for a) ACE-ENA summer, b) ACE-ENA winter, and c) SOCRATES. White dots denote the aircraft flight tracks for the selected cases.
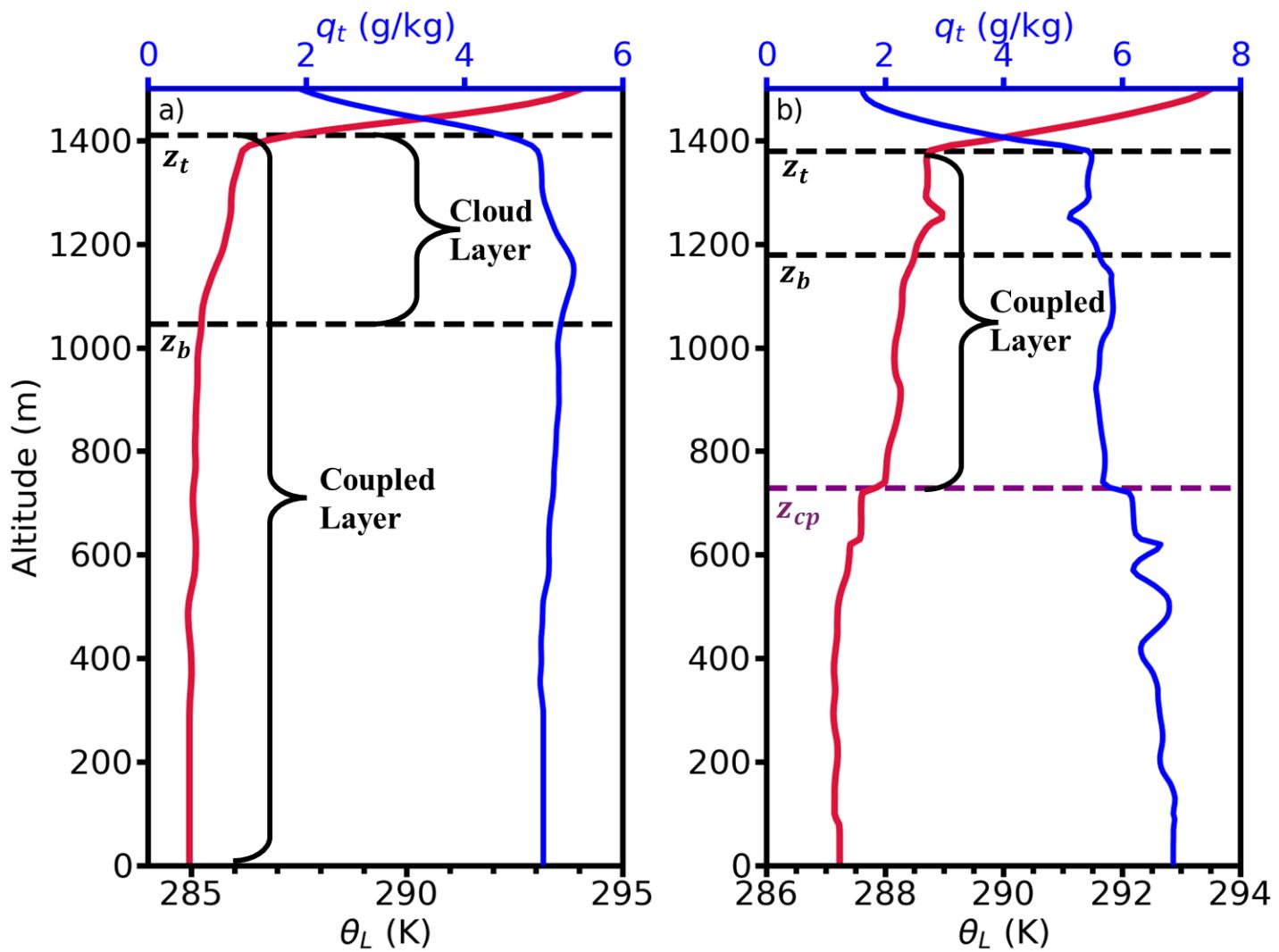
Figure S2. Illustration of coupled layer determination of a) coupled MBL case, and b) decoupled MBL case. Solid lines denote vertical variations of liquid water potential temperature (θ_L, red) and total water mixing ratio (q_t, blue). Black dashed line denotes cloud boundaries and purple dashed line denotes coupled layer base height.
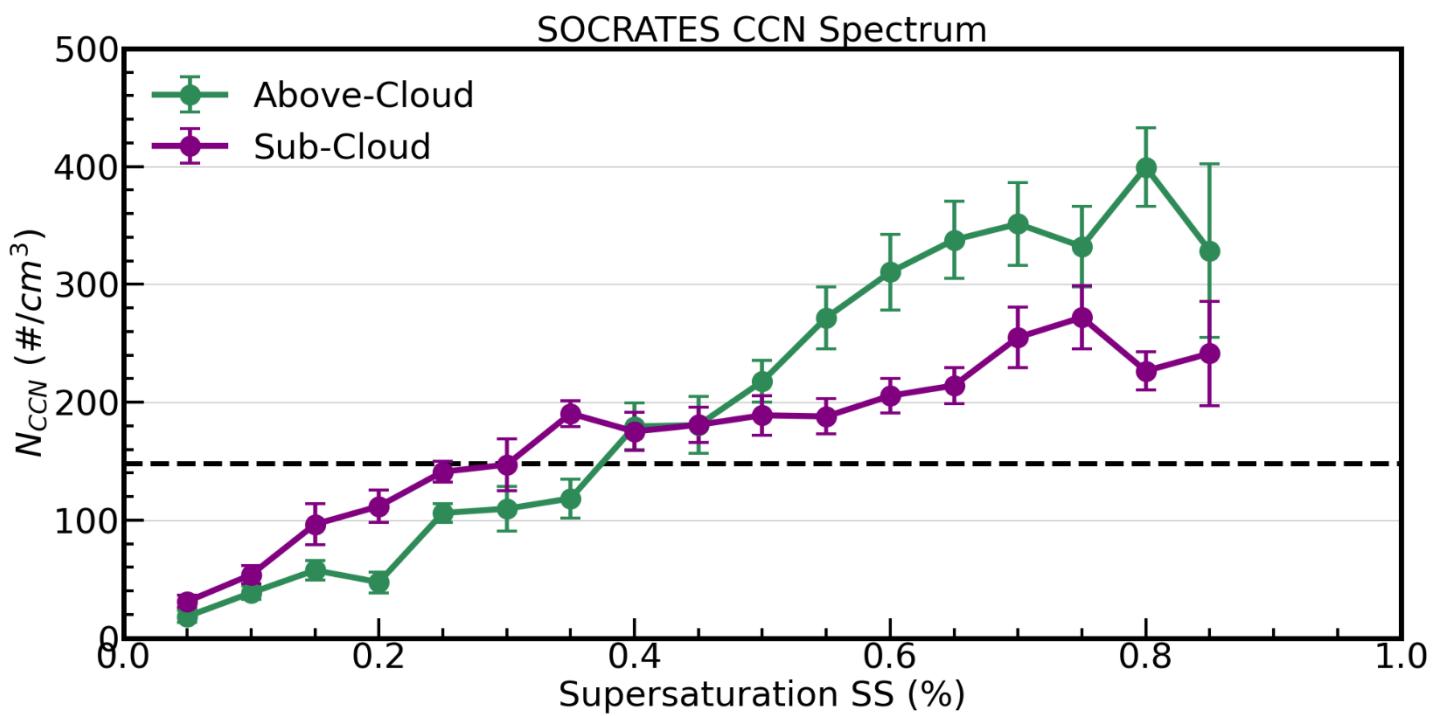
Figure S3. CCN spectra versus supersaturation during SOCRATES for above-cloud (green) and sub-cloud (purple) regimes. Black dashed line denotes the averaged layer-mean N_c. Whisker denotes the standard error of the CCN number concentrations in each supersaturation bin.
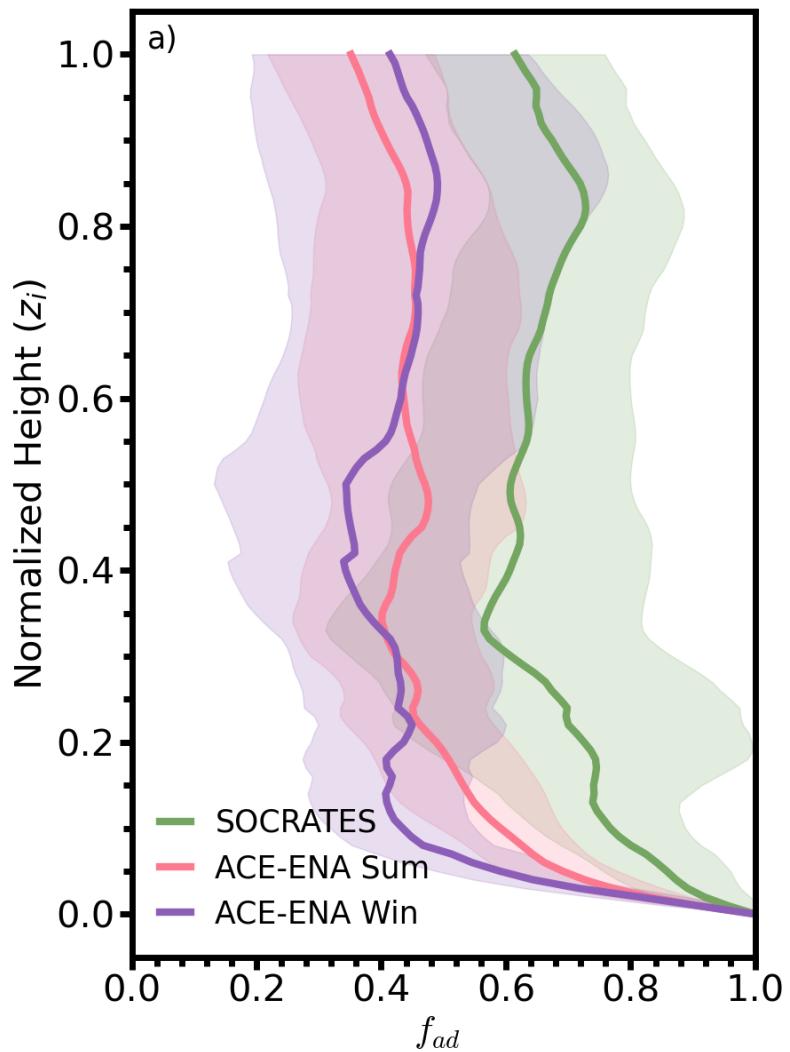
Figure S4. Vertical distributions of in-cloud sub-adiabaticity f_{ad}. Shaded areas denote the inter-cloud-case standard deviations. The ACE-ENA Sum, ACE-ENA Win, and SOCRATES are color-coded with pink, purple, and green, respectively.
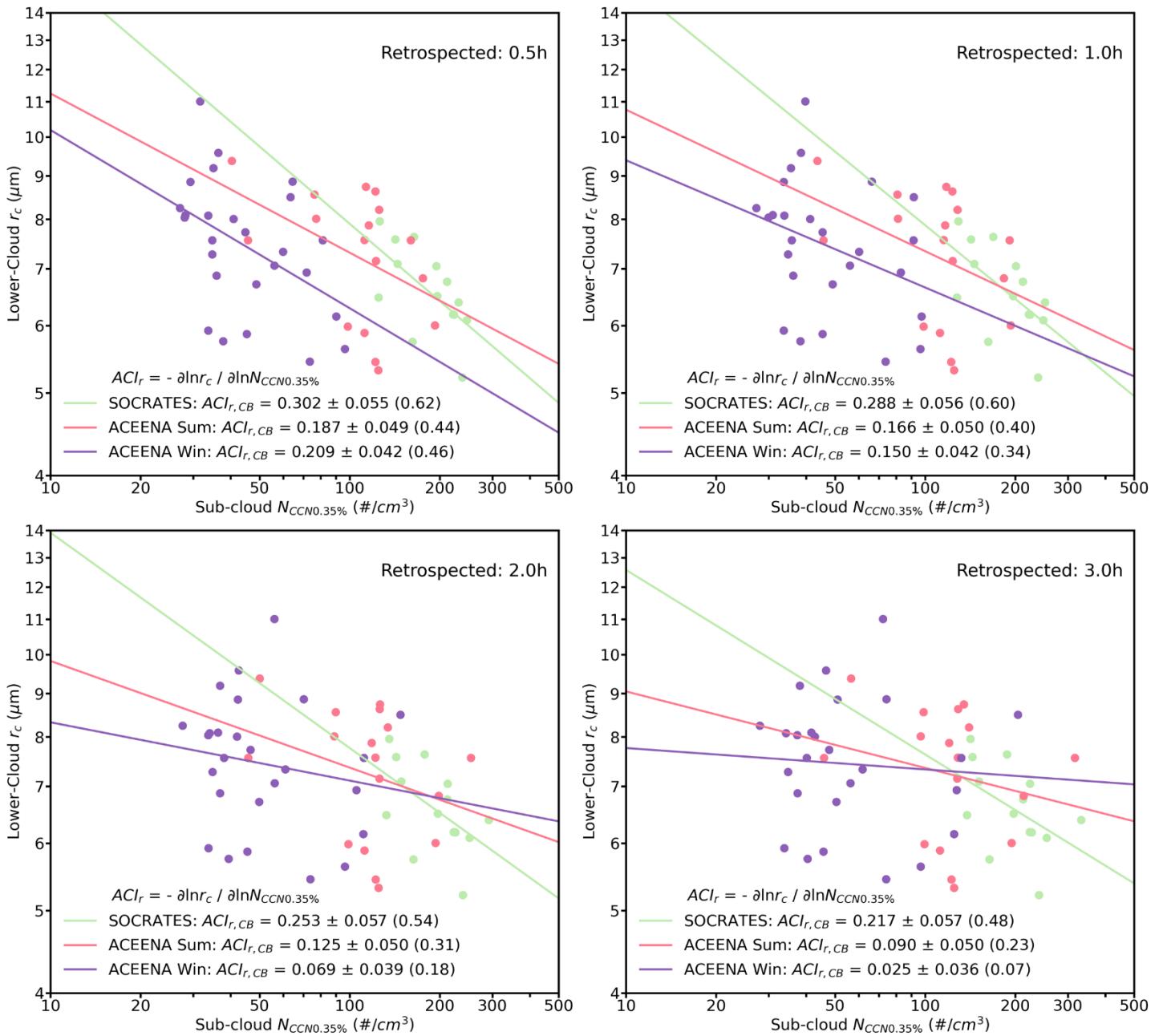
Figure S5. Scatterplots of lower-cloud r_c against the sub-cloud $N_{CCN0.35\%}$, at different $N_{CCN0.35\%}$ retrospective time of a) 0.5 hours, b) 1 hours, c) 2 hours and d) 3 hours. The statistical metrics in the legends denote the ACI values and standard errors, and the absolute values of correlation coefficients (in parentheses). The ACE-ENA Sum, ACE-ENA Win, and SOCRATES are color-coded with pink, purple, and green, respectively.

Table S1. List of selected cloud profiles and associated macrophysics

|				ACE-ENA summer					
Date	Start UTC	End UTC	Precip.*	Cloud base height z_b (m)	Cloud top height z_t (m)	Cloud layer thickness H_c (m)	Coupled layer thickness H_{cp} (m)	Degree of decoupling D_{cp}**	Adiaba-ticity f_{ad}
20170628	9.65	10.8	0	659	797	138	797	0.00	0.35
20170630	9.9	11.3	1	909	1178	269	508	0.74	0.59
20170706	8.95	10.05	1	1151	1607	456	657	0.83	0.41
20170706	10.05	10.3	1	1344	1534	190	424	0.83	0.59
20170706	10.4	11.4	1	1320	1600	280	590	0.77	0.61
20170712	9.5	10.8	1	912	1273	361	593	0.75	0.65
20170712	10.8	11	1	373	597	224	307	0.78	0.77
20170712	11.1	12.3	1	750	1174	424	534	0.85	0.52
20170713	9	10.3	0	1140	1278	138	778	0.44	0.48
20170713	10.3	11.8	0	1169	1345	176	615	0.62	0.54
20170713	11.8	12.55	0	1139	1311	172	591	0.63	0.42
20170715	10.9	12.2	0	918	1080	162	610	0.51	0.44
20170715	12.45	13.6	1	1002	1423	421	613	0.81	0.35
20170718	8.9	9.1	1	627	964	337	964	0.00	0.85
20170718	9.1	10.9	1	588	1080	492	1080	0.00	0.67
20170718	10.9	11.9	1	646	970	324	970	0.00	0.69
20170720	9	10.8	1	233	1124	891	1124	0.00	0.47
20170720	10.8	11.1	1	546	1145	599	855	0.53	0.36
				ACE-ENA winter					
Date	Start UTC	End UTC	Precip.*	z_b	z_t	H_c	H_{cp}	D_{cp}**	f_{ad}
20180119	12.8	14.1	1	405	1009	604	1009	0.00	0.18
20180119	14.3	15.5	1	441	984	543	984	0.00	0.37
20180119	15.5	15.7	1	666	967	301	497	0.71	0.39
20180121	10.3	11.4	1	1113	1399	286	799	0.54	0.5
20180121	11.45	11.7	0	1152	1225	73	805	0.36	0.61
20180125	11.5	12.7	1	1191	1613	422	483	0.95	0.86
20180125	12.7	13	1	1235	1663	428	1663	0.00	0.89
20180125	13	14.1	1	1102	1655	553	755	0.81	0.73
20180126	11.1	11.2	0	1046	1410	364	1410	0.00	0.54
20180126	11.3	11.55	0	1104	1410	306	1410	0.00	0.45
20180126	11.55	13	0	1102	1494	392	1494	0.00	0.46
20180129	10.1	11.3	1	1180	1379	199	649	0.62	0.44
20180129	11.6	13	1	1077	1429	352	679	0.70	0.32
20180130	10.1	11.8	0	941	1396	455	1396	0.00	0.75
20180130	11.8	12.2	0	1034	1212	178	242	0.94	0.67
20180130	12.2	13.4	0	1056	1376	320	346	0.98	0.78
20180130	13.4	13.6	0	1214	1331	117	1201	0.11	0.75
20180207	17.9	18.8	0	1158	1512	354	1512	0.00	0.36
20180208	13.5	14.6	1	1680	2049	369	589	0.87	0.32
20180208	14.6	14.9	0	1925	2061	136	211	0.97	0.3

20180209	13.2	14.6	1	453	802	349	582	0.49	0.49
20180210	15	16.3	0	1371	1546	175	726	0.60	0.32
20180211	11.95	13.55	1	548	1728	1180	1728	0.00	0.22
20180211	13.55	13.8	1	712	1888	1176	1888	0.00	0.11
20180212	11.7	13	0	1043	1287	244	1287	0.00	0.55
20180212	13.25	14.4	0	906	1233	327	1233	0.00	0.39

SOCRATES

Date	Start UTC	End UTC	Precip.*	z_b	z_t	H_c	H_{cp}	D_{cp}**	f_{ad}
20180115	26.0833	26.25	0	2021	2259	238	909	0.67	0.91
20180128	26	26.17	1	741	1336	595	1336	0.00	0.82
20180131	4.667	4.783	1	1112	1599	487	999	0.54	0.55
20180203	27	27.25	1	702	1444	742	1444	0.00	0.39
20180203	27.333	27.5	0	1260	1741	481	1091	0.52	0.60
20180203	27.51	27.625	0	1065	1830	765	1110	0.68	0.52
20180204	26.933	27.367	1	1047	2221	1174	2221	0.00	0.24
20180204	27.417	27.667	1	1295	2256	961	1446	0.63	0.44
20180204	27.683	27.867	1	1759	2355	596	1295	0.60	0.44
20180207	24.833	25.033	0	2167	2397	230	677	0.79	0.80
20180217	27.417	27.7	1	903	1087	184	1087	0.00	0.95
20180217	27.733	27.983	1	907	1303	396	1053	0.28	0.75
20180217	28	28.075	1	820	1298	478	1008	0.35	0.68
20180217	28.075	28.167	1	956	1312	356	912	0.42	0.94
20180217	28.333	28.833	1	1028	1349	321	1349	0.00	0.87
20180217	29.117	29.2	1	752	1324	572	944	0.51	0.66
20180217	29.2	29.267	1	706	1324	618	1324	0.00	0.36
20180219	26.833	26.917	1	577	844	267	844	0.00	0.98
20180219	26.917	26.992	1	476	913	437	913	0.00	0.97
20180219	26.992	27.083	1	468	911	443	911	0.00	0.95
20180219	27.3	27.583	1	696	1045	349	1045	0.00	0.98
20180219	27.75	27.883	1	684	1228	544	918	0.45	0.55
20180219	27.883	27.958	1	646	1259	613	1259	0.00	0.48
20180219	27.958	28.083	1	805	1166	361	936	0.29	0.93
20180219	28.6	28.725	1	821	1119	298	589	0.65	0.92
20180219	28.725	28.817	1	622	1155	533	1155	0.00	0.39
20180219	28.817	28.917	1	855	1101	246	771	0.39	0.77
20180219	29.083	29.333	1	783	1145	362	1145	0.00	0.45

*Precipitation status of 1 means noticeable drizzle droplets ($N_d > 0.001$ cm^{-3}) exists below the cloud base, while 0 means the opposite.

**The degree of MBL decoupling (D_{cp}) is given by $D_{cp} = z_{cp} - z_b$, where $z_{cp} = z_t - H_{cp}$.

Table S2. List of selected cloud profiles and associated microphysics

					ACE-ENA summer							
Date	Start UTC	End UTC	N_c (cm^{-3})	r_c (μm)	LWC_c (g/m^3)	N_d (cm^{-3})	D_{mmd} (μm)	LWC_d (g/m^3)	$N_{CCN,sc}$ (cm^{-3})	$N_{CCN,ac}$ (cm^{-3})	R_{CB} (mm/hr)	L_{CCN} $(cm^{-3}h^{-1})$
20170628	9.65	10.8	66.2	6.3	0.065	0.0058	53.6	0.0006	112.0	104.9	0.0021	-0.05
20170630	9.9	11.3	115.7	6.7	0.130	0.0253	54.4	0.0037	192.3	157.7	0.0055	-0.75
20170706	8.95	10.05	104.9	9.1	0.347	0.4139	51.2	0.0179	108.7	120.0	0.0406	-6.65
20170706	10.05	10.3	71.6	8.1	0.181	0.0362	63.3	0.0030	98.3	117.7	0.0055	-0.39
20170706	10.4	11.4	89.3	9.0	0.264	0.3279	50.9	0.0143	122.4	110.6	0.0616	-5.87
20170712	9.5	10.8	125.6	8.0	0.245	0.0122	65.8	0.0030	73.4	152.6	0.0448	-7.71
20170712	10.8	11	81.8	9.9	0.304	0.1075	71.9	0.0281	120.4	148.4	0.0208	-2.80
20170712	11.1	12.3	86.2	8.7	0.200	0.0528	60.8	0.0093	109.1	142.8	0.0556	-8.56
20170713	9	10.3	143.5	8.1	0.322	0.0075	79.5	0.0036	121.4	133.8	0.0384	-2.20
20170713	10.3	11.8	123.3	5.8	0.093	0.0006	55.3	0.0001	124.7	179.8	0.0012	-0.09
20170713	11.8	12.55	105.2	6.0	0.086	0.0010	56.1	0.0002	121.9	182.0	0.0025	-0.18
20170715	10.9	12.2	34.2	8.5	0.087	0.0313	57.7	0.0037	45.6	30.1	0.0046	-0.09
20170715	12.45	13.6	33.2	12.1	0.205	0.5284	76.1	0.1485	37.2	73.5	0.1255	-6.44
20170718	8.9	9.1	99.0	9.3	0.354	0.0514	79.6	0.0175	114.9	58.3	0.0234	-1.82
20170718	9.1	10.9	81.3	11.4	0.509	0.2273	90.7	0.0991	71.7	53.4	0.1086	-9.05
20170718	10.9	11.9	62.7	11.1	0.369	0.2358	89.2	0.0881	73.2	54.6	0.1698	-8.00
20170720	9	10.8	45.9	10.8	0.180	0.5023	84.4	0.0975	168.0	64.2	0.1854	-15.19
20170720	10.8	11.1	55.5	9.9	0.187	0.3672	101.1	0.1280	128.9	47.6	0.7165	-62.67
					ACE-ENA winter							
Date	Start UTC	End UTC	N_c	r_c	LWC_c	N_d	D_{mmd}	LWC_d	$N_{CCN,sc}$	$N_{CCN,ac}$	R_{CB}	L_{CCN}
20180119	12.8	14.1	20.1	12.0	0.126	0.3981	108.6	0.1495	23.5	31.0	0.6008	-16.24
20180119	14.3	15.5	43.8	11.7	0.263	0.2391	78.8	0.0645	25.0	19.7	0.1591	-8.65
20180119	15.5	15.7	29.8	11.6	0.185	0.4405	69.9	0.0839	34.4	32.6	0.0304	-1.24
20180121	10.3	11.4	49.2	9.3	0.151	0.1644	61.5	0.0206	26.2	33.7	0.0938	-3.72
20180121	11.45	11.7	44.8	8.2	0.095	0.0057	59.0	0.0005	34.7	71.1	0.0031	-0.03
20180125	11.5	12.7	63.8	10.7	0.342	0.1775	76.5	0.0573	35.2	50.2	0.4493	-56.37
20180125	12.7	13	140.9	10.6	0.739	0.0770	98.1	0.0482	62.4	44.8	0.0481	-3.93
20180125	13	14.1	75.9	10.7	0.412	0.1450	93.7	0.0626	60.6	41.7	0.1781	-22.29
20180126	11.1	11.2	110.5	10.5	0.626	0.0698	94.4	0.0312	40.6	47.9	0.0110	-0.71
20180126	11.3	11.55	160.1	9.1	0.579	0.0135	80.9	0.0062	59.4	0.7	0.0097	-0.76
20180126	11.55	13	111.5	9.2	0.408	0.0206	68.8	0.0069	48.4	10.6	0.0102	-0.67
20180129	10.1	11.3	54.8	10.2	0.247	0.0739	60.3	0.0113	34.4	36.0	0.1082	-4.09
20180129	11.6	13	56.1	9.0	0.179	0.0200	61.7	0.0047	33.5	42.3	0.0038	-0.25
20180130	10.1	11.8	82.9	9.2	0.276	0.0993	72.7	0.0184	45.2	58.9	0.0025	-0.15
20180130	11.8	12.2	102.5	9.6	0.396	0.0057	93.0	0.0039	35.6	68.4	0.0037	-0.62
20180130	12.2	13.4	71.9	7.7	0.146	0.0261	61.3	0.0042	33.6	69.5	0.0146	-2.19
20180130	13.4	13.6	58.2	8.8	0.141	0.0097	65.6	0.0031	33.6	75.3	0.0038	-0.05
20180207	17.9	18.8	120.2	8.6	0.359	0.0084	72.7	0.0033	37.2	20.2	0.0173	-1.10
20180208	13.5	14.6	32.3	10.3	0.128	0.2630	74.1	0.0695	25.6	60.6	0.1173	-5.34

Date	Start UTC	End UTC	N_c	r_c	LWC_c	N_d	D_{mmd}	LWC_d	$N_{CCN,sc}$	$N_{CCN,ac}$	R_{CB}	L_{CCN}
20180208	14.6	14.9	59.3	9.8	0.231	0.0086	68.1	0.0023	26.9	62.0	0.0043	-0.37
20180209	13.2	14.6	51.6	11.2	0.337	0.1209	92.7	0.0509	44.2	7.6	0.0169	-1.17
20180210	15	16.3	69.3	7.7	0.159	0.0124	55.4	0.0024	55.9	54.6	0.0030	-0.11
20180211	11.95	13.55	54.0	10.3	0.170	0.3182	100.9	0.1142	71.1	6.3	0.2443	-20.28
20180211	13.55	13.8	50.5	9.2	0.100	0.2453	93.2	0.0313	83.2	1.8	0.1964	-13.91
20180212	11.7	13	126.6	7.9	0.282	0.0058	64.6	0.0012	73.4	92.0	0.0043	-0.23
20180212	13.25	14.4	75.9	6.8	0.108	0.0035	56.3	0.0007	96.3	49.0	0.0018	-0.08
SOCRATES												
Date	Start UTC	End UTC	N_c	r_c	LWC_c	N_d	D_{mmd}	LWC_d	$N_{CCN,sc}$	$N_{CCN,ac}$	R_{CB}	L_{CCN}
20180115	26.0833	26.25	63.4	9.2	0.195	0.4686	51.5	0.0324	−	160.9	0.0157	-0.59
20180128	26	26.17	107.4	9.1	0.269	0.3262	57.2	0.0284	122.9	−	0.0581	-6.25
20180131	4.667	4.783	51.2	10.5	0.217	0.9472	55.1	0.0641	−	−	0.0422	-2.37
20180203	27	27.25	89.0	9.5	0.257	0.4372	51.8	0.0294	−	95.1	0.0147	-1.51
20180203	27.333	27.5	189.1	6.8	0.222	0.0009	47.5	0.0001	−	−	0.0072	-1.35
20180203	27.51	27.625	267.8	6.6	0.258	0.0011	50.0	0.0001	−	−	0.0022	-0.92
20180204	26.933	27.367	101.9	7.3	0.157	0.0685	55.3	0.0048	237.7	59.8	0.0064	-0.78
20180204	27.417	27.667	169.0	7.8	0.261	0.0719	59.9	0.0061	189.4	−	0.0458	-11.57
20180204	27.683	27.867	106.6	7.0	0.146	0.0752	55.7	0.0052	244.9	−	0.0294	-3.25
20180207	24.833	25.033	79.0	6.9	0.107	0.0007	43.9	0.0000	−	−	0.0266	-1.61
20180217	27.417	27.7	157.9	7.6	0.245	0.1240	58.2	0.0125	−	−	0.0031	-0.19
20180217	27.733	27.983	136.5	7.9	0.251	0.1334	54.4	0.0109	143.2	−	0.0234	-2.71
20180217	28	28.075	109.9	8.5	0.263	0.1419	71.4	0.0252	122.4	−	0.0439	-5.15
20180217	28.075	28.167	201.1	8.3	0.418	0.1643	59.4	0.0165	−	198.5	0.0999	-17.65
20180217	28.333	28.833	161.8	7.5	0.237	0.0592	56.0	0.0052	195.8	302.1	0.0072	-0.62
20180217	29.117	29.2	144.9	6.8	0.161	0.0415	59.0	0.0041	211.5	−	0.0020	-0.39
20180217	29.2	29.267	129.2	7.3	0.174	0.0725	69.8	0.0114	211.2	−	0.2970	-40.30
20180219	26.833	26.917	124.5	8.1	0.253	0.2345	53.2	0.0174	−	72.9	0.0041	-0.36
20180219	26.917	26.992	159.3	9.1	0.463	0.2569	58.4	0.0261	159.1	−	0.0557	-9.55
20180219	26.992	27.083	169.5	8.7	0.425	0.1897	58.8	0.0182	−	161.0	0.0551	-10.21
20180219	27.3	27.583	163.9	9.7	0.502	0.4954	52.2	0.0372	222.3	−	0.0136	-1.68
20180219	27.75	27.883	140.7	8.1	0.339	0.1568	54.9	0.0121	161.9	75.0	0.0038	-0.72
20180219	27.883	27.958	126.5	8.3	0.330	0.2488	65.9	0.0207	−	23.2	0.0507	-7.02
20180219	27.958	28.083	76.2	9.8	0.315	0.3318	56.7	0.0203	141.7	201.7	0.0104	-0.69
20180219	28.6	28.725	43.1	11.9	0.238	0.7380	54.0	0.0568	−	150.8	0.1010	-4.95
20180219	28.725	28.817	87.5	8.3	0.233	0.4196	68.9	0.0320	−	−	0.0444	-4.03
20180219	28.817	28.917	132.0	7.1	0.172	0.1080	58.0	0.0099	−	132.0	0.0127	-1.20
20180219	29.083	29.333	208.9	7.1	0.256	0.1073	54.6	0.0092	221.2	−	0.0055	-0.81